Available online at www.sciencedirect.com
ScienceDirect
Trans. Nonferrous Met. Soc. China 25(2015) 3546−3552
Transactions of Nonferrous Metals Society of China
www.tnmsc.cn

# Effects of Mn and Sn on microstructure of Al−7Si−Mg alloy modified by Sr and Al−5Ti−B

Ke QIU[1], Ri-chu WANG[1], Chao-qun PENG[1], Nai-guang WANG[2], Zhi-yong CAI[1], Chun ZHANG[1]

1. School of Materials Science and Engineering, Central South University, Changsha 410083, China;
2. School of Metallurgy and Environment, Central South University, Changsha 410083, China

Received 10 August 2015; accepted 22 October 2015

**Abstract:** The effects of Mn and Sn on the microstructure of Al−7Si−Mg alloy modified by Sr and Al−5Ti−B were studied. The results show that the columnar dendrites structure is observed with high content of Sr, indicating a poisoning effect of the Al−5Ti−B grain refinement. In addition, Sr intermetallic compounds distribute on the $TiB_2$ particles, which agglomerate inside the eutectic Si. The mechanism responsible for such poisoning was discussed. The addition of Mn changes the morphology of iron intermetallic compounds from $\beta$-$Al_5FeSi$ to $\alpha$-Al(Mn,Fe)Si. Increasing the amount of Mn changes the morphology of $\alpha$-Al(Mn,Fe)Si from branched shape to rod-like shape with branched distribution, and finally converts $\alpha$-Al(Mn,Fe)Si to Chinese script shape. The microstructure observed by transmission electron microscopy (TEM) shows that Mg is more likely to interact with Sn in contrast with Si under the effect of Sn. $Mg_2Sn$ compound preferentially precipitates between the Si/Si interfaces and Al/Si interfaces.
**Key words:** Al−7Si−Mg aluminum alloy; grain refinement; intermetallic compound; manganese; tin; Al−5Ti−B; Sr

## 1 Introduction

Al−7Si alloys have been widely used in automobile, aircraft, and marine due to their excellent castability, high corrosion resistance, good weldability, and low coefficient of thermal expansion [1−3]. Doping these alloys with Mg effectively improves their mechanical properties by forming fine coherent particles of $Mg_2Si$ during heat treatment.

Various methods are introduced to improve the mechanical properties of these alloys. Chemical modification of eutectic Si is one of the important methods to enhance the mechanical properties of Al−7Si−Mg alloys. The additions of Na, Sr, Y, and Sc can convert the eutectic Si from acicular structure to fine fibers and spherical morphology [4−7]. Sn has a low solid solubility in Al and good tribological property, which favors its application in bearing alloys [8,9]. It has been reported that Sn has cleaning effect on A356 alloys by removing iron and other impurities from solid solution and reducing the volume fraction of iron-rich intermetallics [10]. VIEIRA et al [11] found that adding 0.5% Sn to Al−7Si−Mg alloy could improve its flowing behavior, increase the mould-filling capability, and reduce the liquid segregation. MOHAMED et al [12] reported that A356.2 alloy with addition of 0.05% Sn has better mechanical properties compared with other alloys with different Sn contents.

Fe is an important impurity in Al−Si cast alloys because it always enables the formation of needle-like $\beta$-$Al_5FeSi$ compound during solidification. This intermetallic is detrimental to the mechanical properties and fracture toughness of the alloys due to its sharp edges; therefore, it is easy to have severe stress concentration, leading to the brittleness of the alloys [13]. Mn is the most commonly used element for replacing the acicular $\beta$-$Al_5FeSi$ phase with $\alpha$-Al(Mn,Fe)Si phase, and hence reduces the harmful impact of impurity compound. However, the morphology of this $\alpha$-phase depends on Mn content, which determines the formation of Chinese script, granular, and polyhedral morphologies [14,15]. With the low ratio of Mn to Fe, the pastes of $\beta$-$Al_5FeSi$ phase convert to granular or Chinese script morphology, but this intermetallic compound turns to be polyhedral or star-like shape if the content of Mn is high.

The data available on the individual addition of Mn or Sn in Al−7Si−Mg alloys are enough, whereas less

**Corresponding author:** Ri-chu WANG; Tel: +86-731-88836638; E-mail: rcwcsu@163.com
DOI: 10.1016/S1003-6326(15)64075-4

attention has been paid to the combined addition of Mn and Sn. The aim of this work is to investigate the influence of combined addition of Mn and Sn on the microstructure of Al−7Si−Mg alloy modified by Sr. The evolution of intermetallic compounds with different amounts of Mn and Sn additions is studied, and the effect of these minor elements on the grain refinement of Al−5Ti−B alloy is also discussed.

## 2 Experimental

Ternary Al−7Si−0.35Mg alloy was prepared from commercial purity Al, Mg and Al−22Si master alloy in 4 kg capacity using SiC crucibles in an electric resistance furnace, which was held at a constant temperature of (750±5) °C. The melt was covered by cover agent. Al−10Sr master alloy was added to ensure that the mass fraction of Sr in the melt reached $3\times10^{-5}$ and $3\times10^{-4}$. Al−5Ti−B master alloy was chosen as the grain refiner. The mass fraction of the added grain refiner in each alloy was 0.5%. To study the combined effect of Mn and Sn, Al−15Mn master alloy and commercial pure Sn were added to obtain the desired levels. The melt was thoroughly stirred with pure carbon rod and degassed with hexachlorothane. The holding time was over 15 min for enough incubation of Sr modification. The molten metal was poured into an L-shaped rectangular ZnO-coated metallic mold preheated at 250 °C. The as-cast alloy was subjected to T6 heat treatment including 8 h solution at 540 °C followed by water quenching, and 6 h aging at 160 °C.

The alloy compositions are given in Table 1. The microstructure features of these alloys were studied by optical microscopy (OM) after the samples were etched with an aqueous solution of 0.5% HF. The un-etched samples were examined by scanning electron microscopy (SEM) with energy dispersive spectroscopy (EDS). Moreover, electron probe microanalysis (EPMA) was employed for mapping and analyzing the micro-constituents of intermetallic phases. Precipitates of the samples were analyzed by transmission electron microscopy (TEM). TEM thin foils were prepared by the combination of mechanical pitting and ion beam thinning at 5 kV.

**Table 1** Chemical compositions of various alloys (mass fraction, %)

| Alloy | Si | Mg | Fe | Mn | Sn | Sr | Al |
|---|---|---|---|---|---|---|---|
| M1 | 6.95 | 0.33 | 0.53 | 0.001 | 0.001 | 0.003 | Bal. |
| M2 | 6.96 | 0.32 | 0.51 | 0.001 | 0.001 | 0.003 | Bal. |
| MS1 | 6.98 | 0.33 | 0.48 | 0.32 | 0.48 | 0.03 | Bal. |
| MS2 | 6.98 | 0.33 | 0.51 | 0.51 | 0.09 | 0.03 | Bal. |

## 3 Results and discussion

### 3.1 Effect of grain refinement induced by Mn, Sn, and Sr

The as-cast microstructure of $3\times10^{-5}$ Sr-modified alloy (denoted as M1, without grain refinement) is shown in Fig. 1(a). The morphology of this alloy is characterized by columnar dendrites together with interdendritic Al−Si eutectic. With the addition of 0.5% Al−5Ti−B grain refiner, a thin $TiAl_3$ layer has an affinity to segregate onto the surface of $TiB_2$ and these duplex particles act as the nucleation sites. Hence, the columnar dendrites transform into equiaxed dendrites, as shown in Fig. 1(b) [16,17]. Figures 1(c) and (d) depict the morphologies of MS1 and MS2 alloys containing different amounts of Mn and Sn, respectively. The grain sizes of $\alpha$(Al) are larger in both alloys compared with M1 and M2 alloys. The increase of grain size is observed with the high Sr addition ($3\times10^{-4}$). Increasing Sr content decreases the eutectic temperature and enlarges the solidification zone [18,19]. As a result, the primary $\alpha$(Al) fully grows after nucleation and the grain sizes are coarsened. However, the grain refinement appears to be fading because both alloys are characterized by the columnar dendrites.

Figure 2 shows the back scattered electron image of the as-cast MS2-T6 alloy and the quantitative analyses at four different locations are shown in Table 2. Some particles distribute in the eutectic Si region and the rod-like intermetallic phases also exist in the alloy. The chemical compositions of the particles in Fig. 2 verified by EPMA demonstrate that these particles are $TiB_2$ and the intermetallics are Al(Mn,Fe)Si and $Mg_2Sn$−Sn eutectic [12]. $TiB_2$ particles do not act as the substrate for nucleation of $\alpha$(Al), instead, they agglomerate in eutectic Si region.

$TiB_2$ interface is an energetically favorable site for Si and the surface energy factors adversely affect the $TiB_2$ as a nucleation site [20]. During the solidification of Al−7Si alloy, $TiB_2$ particles distribute in the interdendritic spaces and cannot serve as the nucleation site for the $\alpha$(Al) phase alone [16]. A thin $TiAl_3$ layer has an affinity to segregate onto the surface of $TiB_2$ and these duplex particles act as the nucleation sites [16,17]. It has been reported that $Ti_5Si_3$ forms on the surface of $TiAl_3$ and causes the poisoning effect of Al−Ti−B grain refiners in Al−Si casting alloys [21]. However, other reports suggested that the formation of $TiSi_2$ compound is the main reason for poisoning [22,23]. It is agreed that increasing the amount of grain refiner could overcome the fading behavior. The equiaxed dendrites in Fig. 1(b) indicate that the amount of Al−5Ti−B intermediate alloy is enough for the grain refinement. The poisoning

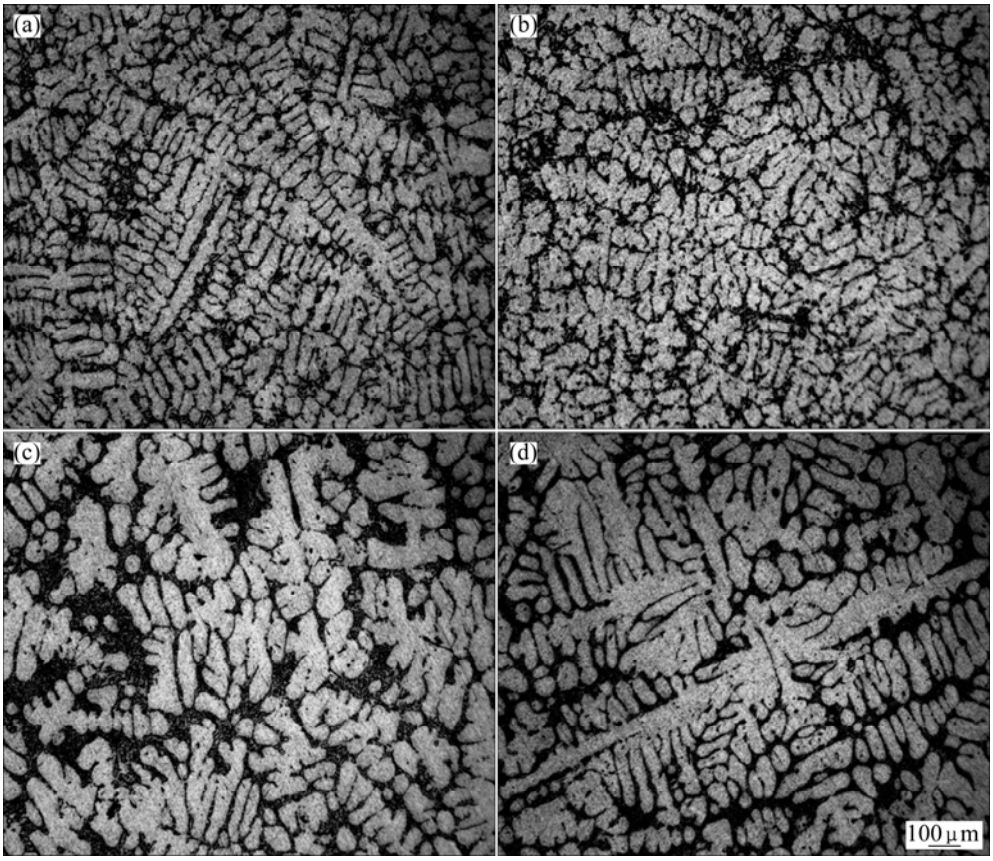


**Fig. 1** Optical micrographs of M1 (a), M2 (b), MS1 (c), and MS2 (d) alloys in as-cast condition

**Table 2** Phase compositions in Fig. 2 (mass fraction, %)

| Zone No. in Fig. 2 | Al | Si | Mg | Fe | Sn | Mn | Ti | B | Sr |
|---|---|---|---|---|---|---|---|---|---|
| 1 | 9.1678 | 3.6653 | 2.1760 | 0.0088 | 43.7219 | 0.0442 | 18.6673 | 22.3766 | 0.1722 |
| 2 | 2.4563 | 0.1854 | 1.8502 | 0.0189 | 11.0181 | 0.0471 | 31.0152 | 53.3761 | 0.0326 |
| 3 | 38.0240 | 0.3826 | 3.7222 | 0.0253 | 36.1323 | 0.2133 | 10.6539 | 10.6730 | 0.1734 |
| 4 | 75.4032 | 7.5383 | 0.9823 | 0.0044 | 15.9964 | 0.0754 | − | − | − |

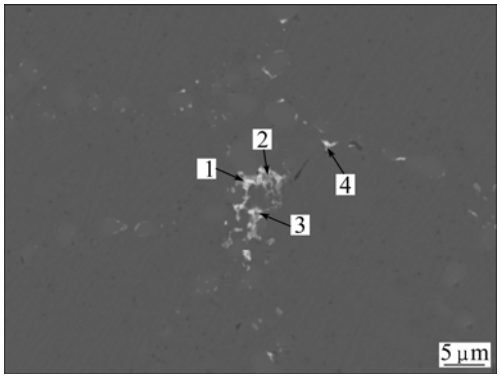


**Fig. 2** Back scattered electron micrograph of MS2 alloy after T6 condition

behavior shown in Figs. 1(c) and (d) indicates the same levels of Al−5Ti−B as M2 alloy; however, these are not adequate for MS1 and MS2 alloys. To analyze the poisoning phenomenon of grain refinement, X-ray mapping in Fig. 2 is conducted to determine the distribution of Ti, B and Sr, as shown in Fig. 3. It can be seen that some Sr element absorbs on the Si crystal but also agglomerates and drops onto the $TiB_2$ particles. Sr is completely miscible in the base alloy and would not be expected to settle down unless it combines with other elements to form dense compounds [24]. Therefore, there must be the formation of Sr compound due to the observation of agglomeration of Sr. $TiB_2$ particles are thought to be stable and no interaction between $TiB_2$ and Sr has been reported. LIAO et al [25] assumed that there is an interaction between Sr and Ti to poison the modification. In contrary, SAMUEL et al [26] supposed that Sr and Ti do not interact with each other to weaken the Si modification.

The well-modified structures in Figs. 1(c) and (d) show that the amount of Al−5Ti−B does not poison the Sr modification. The observation of Sr compound in

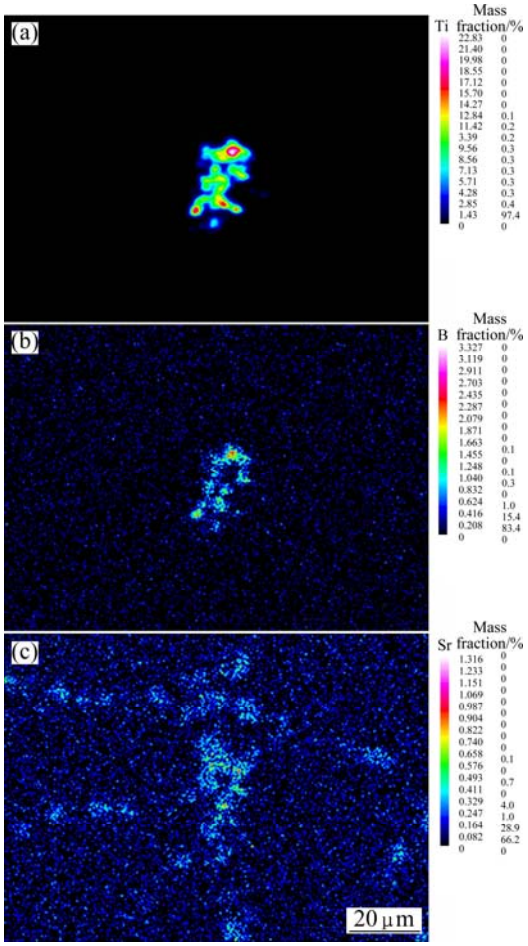


**Fig. 3** X-ray mapping in Fig. 2 showing elements distribution: (a) Ti; (b) B; (c) Sr

Fig. 3 shows that some excess Sr interacts with other elements. It is impossible to quantitatively measure the reliable composition of Sr compound by EPMA as these particles are extremely small. It is assumed that the formation of Sr-compound may be one of the reasons for poisoning grain refinement. It has been reported that $1\times10^{-4}$ Sr is enough for modification of the eutectic Si [18]. In this work, $3\times10^{-4}$ Sr was added to refine the Si particles. It is considered that the excess Sr interacts with Ti, leading to the reduction of Ti content in the melt. As the amount of Al−5Ti−B is not quite adequate for the grain refinement, once the interaction occurs, the resident amount of Ti is not enough for the formation of $TiAl_3$ layer onto $TiB_2$ particles due to the interaction of Ti and Si. However, LU and DAHLE [24] found that good modification and grain refinement occur with the addition of $3.5\times10^{-4}$ Sr and Al−5Ti−B grain refiner in the hypoeutectic Al−Si alloys. It might be attributed to the fact that their addition levels of grain refiners are much higher. Since no interactions between Mn and Sr, Sn and Sr have been reported, the interaction between Sr and Ti needs to be further investigated to identify the chemical composition and nucleation mechanism.

### 3.2 Effect of Mn on precipitation of Al(Mn,Fe)Si

In the absence of Mn and Sn, the iron intermetallic compounds are the long and needle-like $\beta$-$Al_5FeSi$ in the alloy, as shown in Fig. 4. It can be seen that the $\beta$-phases are branching out from the eutectic region across the matrix. Figure 5 shows the microstructures of MS1 and MS2 alloys with 0.32% and 0.51% Mn additions, 0.48% and 0.09% Sn additions after T6 condition. It is seen that the needle-like Fe-intermetallic phases have been

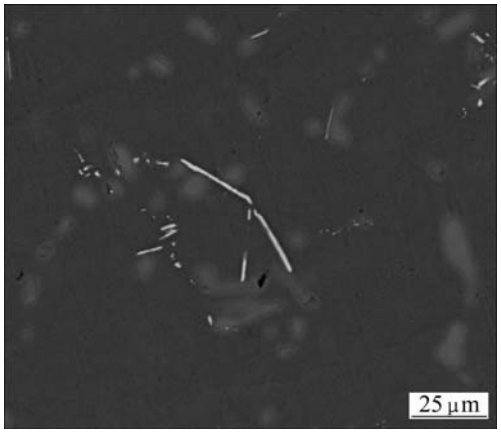


**Fig. 4** Microstructure of intermetallic compounds of Al−7Si−Mg alloy without Mn and Sn addition after T6 condition

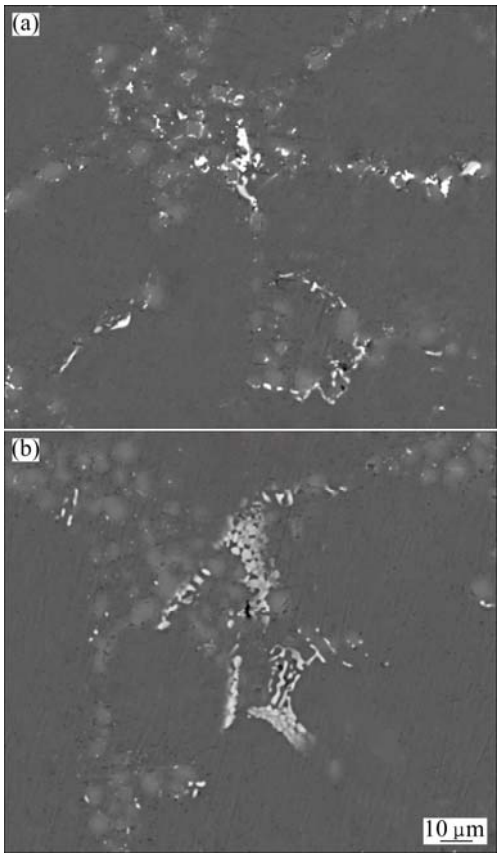


**Fig. 5** SEM images showing intermatllic compounds with different composition of alloys after T6 codition: (a) MS1 alloy; (b) MS2 alloy

replaced by the polyhedral and granular $\alpha$-Al(Mn, Fe)Si phases, while the $\beta$-Sn phases are performed to both large round morphology and small particles within the eutectic regions. Compared with MS1 and MS2 alloys in Fig. 5, even Mn contents are lower in MS1 alloy, more intermetallic phases within the eutectic region can be observed because the Sn contents are higher. When Mn content is 0.32% (MS1 alloy), the Fe-intermetallic appears to be rod-like morphology with branched distribution in the alloy.

Iron rich intermetallics with higher Mn levels, according to SHABESTARI et al [27], exhibit as needle-like $\alpha$-phase forms, which seems to be consistent with Fig. 5(a) in the present work. As the Mn content increases to the level up to 0.51%, the large Chinese scripts $\alpha$-phase in Fig. 5(b) indicates that by increasing the addition amount of Mn, the $\beta$-$Al_5FeSi$ firstly converts to $\alpha$-phase in a branched shape and finally large $\alpha$-phase Chinese scripts morphology. This phenomenon is in agreement with the results observed by SEIFEDDINE et al [13]. It has been reported that the rod-like $\alpha$-Al(Mn,Fe)Si phase would form near the eutectic Si temperature with the addition of low content of Mn in A356−0.2Fe alloy, while increasing the ratio of Mn to Fe up to 1.0, the $\alpha$-Al(Mn,Fe)Si phase can form at higher temperature than eutectic Si particles and thus the rod-like morphology would convert to skeleton shape [14].

The microstructure evolution of iron rich intermetallics with Mn concentration in the present work is described as follows. At low Mn concentrations, $\beta$-$Al_5FeSi$ phases would convert to branched $\alpha$-Al(Mn,Fe)Si. As the content of Mn increases, small rod-like $\alpha$-phases would form but still distribute in discontinuous branched morphology. At an appropriate ratio of Mn to Fe, Chinese script $\alpha$-phase will form; however, this certain critical ratio of Mn to Fe depends on the cooling rate.

### 3.3 Effect of Sn on $\beta$-Sn and $Mg_2Sn$

Figure 5(a) demonstrates that the $\beta$-Sn phases are gathered and spheroidized inside the eutectic Si regions. The reason is attributed to the low solubility of Sn in both Al and Si. In the eutectic Al−Si−Sn system, there is no compound formation other than $\alpha$(Al), Si and $\beta$-Sn. Thus, $\beta$-Sn is the last solidified phase and preferentially locates at the Al−Si interface and inside the eutectic Si regions at the end of solidification.

Mg has higher affinity for Si and Sn than for Al, and can form binary intermetallics with Al after these elements are completely combined. However, there are different opinions about the formation of Mg intermetallic compounds with the addition of Sn. KLIAUGA and FERRANTE [28] supposed that Sn presents as small globules and acts as a substrate for $Mg_2Si$ precipitation. In their subsequent work, they did not observe either $Mg_2Sn$ or $Mg_2Si$, but they believed that $Mg_2Si$ must have formed according to their SEM and DSC measurements [10]. MOHAMED et al [12] supposed that the formation of $Mg_2Sn$ is the result of the reaction among the Al, $Mg_2Si$, $Mg_5Al_8$, and Sn. According to their theory, the formation of $Mg_2Sn$ without excess Mg is only possible with partial (or complete) anions and with isovalent replacement of Si in $Mg_2Si$ with Sn. In the present work, TEM observation of the MS1 alloy after heat treatment is shown in Fig. 6 to identify the precipitation of Mg. It can be seen that there are small particles distributing between Si/Si interfaces and Al/Si interfaces. X-ray mapping indicates that these small particles are $Mg_2Sn$ precipitates. It seems that Sn tends to interact with Mg more easily than Si, which is consistent with Ref. [12]. However, the morphology of $Mg_2Sn$ in this work is not the same as Ref. [12]. The $Mg_2Sn$ phases do not exhibit Chinese scripts morphology but small particles between Si/Si and Al/Si interfaces, while the excess Sn will form $\beta$-Sn inside the eutectic

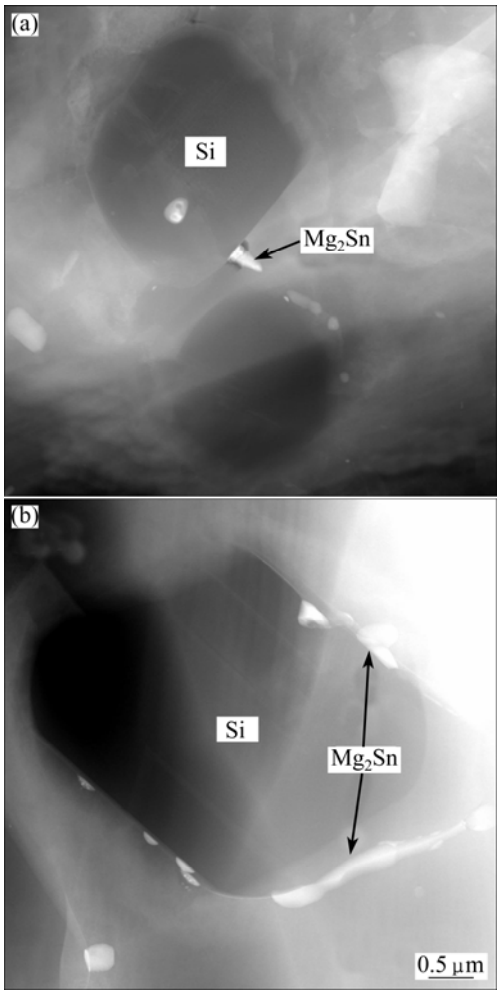


**Fig. 6** TEM images of MS1 alloy showing $Mg_2Sn$ precipitation: (a) Si/Si interface; (b) Al/Si interface

regions. The difference among the observation of Mg intermetallics by several studies is still unclear and needs to be further investigated.

## 4 Conclusions

1) Poisoning of Al−5Ti−B grain refiners was observed in higher Sr content alloys, which indicates that an interaction occurs between Sr and Ti, resulting in the reduction of the amount of $TiAl_3$ in the melt and causing the fading behavior.

2) Addition of Mn can change the iron intermetallics from $\beta$-AlFeSi to $\alpha$-Al(Mn,Fe)Si. The increasing Mn content leads to the evolution of $\alpha$-phase morphology first into branched shape, then into small rod-like structure with branched shape distribution, and finally into Chinese scripts shape.

3) Addition of Sn into Al−7Si−Mg alloy may prevent the formation of $Mg_2Si$, but Sn precipitates as $Mg_2Sn$ phases between Si/Si interfaces and Al/Si interfaces.

## Acknowledgments

The authors would like to gratefully thank Dr. Yan GUO for valuable discussion about this project, as well as his intellectual contribution and support through the course of this research.

## References

[1] KAUFMAN J G. Introduction to aluminum alloys and tempers [M]. Geauga: ASM International, 2000.

[2] BASAVAKUMAR K G, MUKUNDA P G, CHAKRABORTY M. Influence of grain refinement and modification on microstructure and mechanical properties of Al−7Si and Al−7Si−2.5Cu cast alloys [J]. Materials Characterization, 2008, 59: 283−289.

[3] CHEN Rui, SHI Yu-feng, XU Qing-gan, LIU Bai-cheng. Effect of cooling rate on solidification parameters and microstructure of Al−7Si−0.3Mg−0.15Fe alloy [J]. Transactions of Nonferrous Metals Society of China, 2014, 24(6): 1645−1652.

[4] HEGDE S, PRABHU K N. Modification of eutectic silicon in Al−Si alloys [J]. Journal of Materials Science, 2008, 43: 3009−3027.

[5] LI B, WANG H, JIE J, WEI Z. Effects of yttrium and heat treatment on the microstructure and tensile properties of Al−7.5Si−0.5Mg alloy [J]. Materials & Design, 2011, 32: 1617−1622.

[6] ZHANG W, LIU Y, YANG J, DANG J, XU H, DU Z. Effects of Sc content on the microstructure of as-cast Al−7wt.% Si alloys [J]. Materials Characterization, 2012, 66: 104−110.

[7] SUN Shao-chun, YUAN Bo, LIU Man-ping. Effects of moulding sands and wall thickness on microstructure and mechanical properties of Sr-modified A356 aluminum casting alloy [J]. Transactions of Nonferrous Metals Society of China, 2012, 22(8): 1884−1890.

[8] LIU X, ZENG M Q, MA Y, ZHU M. Wear behavior of Al−Sn alloys with different distribution of Sn dispersoids manipulated by mechanical alloying and sintering [J]. Wear, 2008, 265: 1857−1863.

[9] YUAN G C, LI Z J, LOU Y X, ZHANG X M. Study on crystallization and microstructure for new series of Al−Sn−Si alloys [J]. Materials Science and Engineering A, 2000, 280: 108−115.

[10] KLIAUGA A, VIEIRA E, FERRANTE M. The influence of impurity level and tin addition on the ageing heat treatment of the 356 class alloy [J]. Materials Science and Engineering A, 2008, 480: 5−16.

[11] VIEIRA E A, KLIAUGA A M, FERRANTE M. Microstructural evolution and rheological behaviour of aluminium alloys A356, and A356+0.5% Sn designed for thixocasting [J]. Journal of Materials Processing Technology, 2004, 155−156: 1623−1628.

[12] MOHAMED A M A, SAMUEL F H, SAMUEL A M, DOTY H W, VALTIERRA S. Influence of tin addition on the microstructure and mechanical properties of Al−Si−Cu−Mg and Al−Si−Mg casting alloys [J]. Metallurgical and Materials Transactions A, 2008, 39: 490−501.

[13] SEIFEDDINE S, JOHANSSON S, SVENSSON I L. The influence of cooling rate and manganese content on the $\beta$-Al5FeSi phase formation and mechanical properties of Al−Si-based alloys [J]. Materials Science and Engineering A, 2008, 490: 385−390.

[14] KIM H Y, PARK T Y, HAN S W, LEE H M. Effects of Mn on the crystal structure of $\alpha$-Al(Mn,Fe)Si particles in A356 alloys [J]. Journal of Crystal Growth, 2006, 291: 207−211.

[15] ZAHEDI H, EMAMY M, RAZAGHIAN A, MAHTA M, CAMPBELL J, TIRYAKIOĞLU M. The effect of Fe-rich intermetallics on the weibull distribution of tensile properties in a cast Al-5 Pct Si-3 Pct Cu-1 Pct Fe-0.3 Pct Mg Alloy [J]. Metallurgical and Materials Transactions A, 2007, 38: 659−670.

[16] MOHANTY P S, GRUZLESKI J E. Grain refinement mechanisms of hypoeutectic Al−Si alloys [J]. Acta Materialia, 1996, 44: 3749−3760.

[17] SCHUMACHER P, GREER A L, WORTH J, EVANS P V, KEARNS M A, FISHER P, GREEN A H. New studies of nucleation mechanisms in aluminium alloys: Implications for grain refinement practice [J]. Materials Science and Technology, 1998, 14: 394−404.

[18] KIM J H, CHOI J W, CHOI J P, LEE C H, YOON E P. A study on the variation of solidification contraction of A356 aluminum alloy with Sr addition [J]. Journal of Materials Science Letters, 2000, 19: 1395−1398.

[19] NAFISI S, GHOMASHCHI R. Effects of modification during conventional and semi-solid metal processing of A356 Al−Si alloy [J]. Materials Science and Engineering A, 2006, 415: 273−285.

[20] RAVI K R, MANIVANNAN S, PHANIKUMAR G, MURTY B S, SUNDARRAJ S. Influence of mg on grain refinement of near eutectic Al−Si alloys [J]. Metallurgical and Materials Transactions A, 2011, 42: 2028−2039.

[21] QIU D, TAYLOR J A, ZHANG M X, KELLY P M. A mechanism for the poisoning effect of silicon on the grain refinement of Al−Si alloys [J]. Acta Materialia, 2007, 55: 1447−1456.

[22] SCHUMACHER P, MCKAY B J. TEM investigation of heterogeneous nucleation mechanisms in Al−Si alloys [J]. Journal of Non-Crystalline Solids, 2003, 317: 123−128.

[23] QUESTED T E, DINSDALE A T, GREER A L. Thermodynamic evidence for a poisoning mechanism in the Al−Si−Ti system [J]. Materials Science and Technology, 2006, 22: 1126−1134.

[24] LU L, DAHLE A K. Effects of combined additions of Sr and AlTiB grain refiners in hypoeutectic Al−Si foundry alloys [J]. Materials Science and Engineering A, 2006, 435−436: 288−296.

[25] LIAO H, SUN Y, SUN G. Effect of Al−5Ti−1B on the microstructure of near-eutectic Al−13.0%Si alloys modified with Sr [J]. Journal of Materials Science, 2002, 37: 3489−3495.

[26] SAMUEL A M, DOTY H W, VALTIERRA S, SAMUEL F H. Effect of grain refining and Sr-modification interactions on the impact toughness of Al−Si−Mg cast alloys [J]. Materials & Design, 2014, 56: 264−273.

[27] SHABESTARI S, MAHMUDI T, EMAMY M, CAMPBELL T. Effect of Mn and Sr on intermetallics in Fe-rich eutectic Al−Si alloy [J]. International Journal of Cast Metals Research, 2002, 15: 17−24.

[28] KLIAUGA A, FERRANTE M. The effect of Sn additions on the semi-solid microstructure of an Al−7Si−0.3 Mg alloy [J]. Materials Science and Engineering A, 2002, 337: 67−72.

# Mn 和 Sn 对 Sr 变质、Al−5Ti−B 晶粒细化 Al−7Si−Mg 合金显微组织的影响

邱 科[1]，王日初[1]，彭超群[1]，王乃光[2]，蔡志勇[1]，张 纯[1]

1. 中南大学 材料科学与工程学院，长沙 410083;
2. 中南大学 冶金与环境学院，长沙 410083

**摘 要**：研究 Mn 与 Sn 对 Sr 变质、Al−5Ti−B 晶粒细化 Al−7Si−Mg 合金显微组织的影响。结果表明，合金添加高含量 Sr 后具有柱状树枝晶结构，Al−5Ti−B 晶粒细化剂发生了毒化现象：$TiB_2$ 颗粒偏聚在共晶 Si 区域，并发现 Sr 金属间化合物在 $TiB_2$ 颗粒上分布。讨论了 Sr 毒化现象的机理。此外，添加 Mn 元素会使合金的富铁相结构从 $\beta$-$Al_5FeSi$ 向 $\alpha$-Al(Mn,Fe)Si 转变。随着 Mn 含量的增加，$\alpha$-Al(Mn,Fe)Si 相从树枝状转变为树枝状分布的小棒状，最终转变为汉字状结构。透射电镜(TEM)观察显示，Mg 相对于 Si 更倾向于与 Sn 反应，$Mg_2Sn$ 在 Si/Si 界面或 Al/Si 界面上析出。

**关键词**：Al−7Si−Mg 铝合金；晶粒细化；金属间化合物；锰；锡；Al−5Ti−B；锶

**(Edited by Yun-bin HE)**